



RESEARCH ARTICLE

In Vivo ¹⁸F-APN-1607 Tau Positron Emission Tomography Imaging in *MAPT* Mutations: Cross-Sectional and Longitudinal Findings

Xin-Yue Zhou, MD, PhD,¹ Jia-Ying Lu, MD,² Feng-Tao Liu, MD, PhD,¹  Ping Wu, MD, PhD,² Jue Zhao, MD, PhD,¹ Zi-Zhao Ju, MD,² Yi-Lin Tang, MD, PhD,¹ Qing-Yi Shi, MD,² Hua-Mei Lin, MD,² Jian-Jun Wu, MD, PhD,¹ Tzu-Chen Yen, MD, PhD,³ Chuan-Tao Zuo, MD, PhD,^{2*} Yi-Min Sun, MD, PhD,^{1*} and Jian Wang, MD, PhD^{1*} 

¹Department of Neurology and National Research Center for Aging and Medicine & National Center for Neurological Disorders, State Key Laboratory of Medical Neurobiology, Huashan Hospital, Fudan University, Shanghai, China

²PET Center, Huashan Hospital, Fudan University, Shanghai, China

³APRINOIA Therapeutics Co., Ltd, Suzhou, China

ABSTRACT: Background: Frontotemporal lobar degeneration with tauopathy caused by *MAPT* (microtubule-associated protein tau) mutations is a highly heterogeneous disorder. The ability to visualize and longitudinally monitor tau deposits may be beneficial to understand disease pathophysiology and predict clinical trajectories.

Objective: The aim of this study was to investigate the cross-sectional and longitudinal ¹⁸F-APN-1607 positron emission tomography/computed tomography (PET/CT) imaging findings in *MAPT* mutation carriers.

Methods: Seven carriers of *MAPT* mutations (six within exon 10 and one outside of exon 10) and 15 healthy control subjects were included. All participants underwent ¹⁸F-APN-1607 PET/CT at baseline. Three carriers of exon 10 mutations received follow-up ¹⁸F-APN-1607 PET/CT scans. Standardized uptake value ratio (SUVR) maps were obtained using the cerebellar gray matter as the reference region. SUVR values observed in *MAPT* mutation carriers were normalized to data from healthy control subjects. A regional SUVR z score ≥ 2 was used as the criterion to define positive ¹⁸F-APN-1607 PET/CT findings.

Results: Although the seven study patients had heterogeneous clinical phenotypes, all showed a significant ¹⁸F-APN-1607 uptake characterized by high-contrast signals. However, the anatomical localization of tau deposits differed in patients with distinct clinical symptoms. Follow-up imaging data, which were available for three patients, demonstrated worsening trends in patterns of tau accumulation over time, which were paralleled by a significant clinical deterioration.

Conclusions: Our data represent a promising step in understanding the usefulness of ¹⁸F-APN-1607 PET/CT imaging for detecting tau accumulation in *MAPT* mutation carriers. Our preliminary follow-up data also suggest the potential value of ¹⁸F-APN-1607 PET/CT for monitoring the longitudinal trajectories of frontotemporal lobar degeneration caused by *MAPT* mutations. © 2021 International Parkinson and Movement Disorder Society

Key Words: *MAPT*; frontotemporal lobar degeneration; ¹⁸F-APN-1607; tau PET; disease course

Frontotemporal lobar degeneration (FTLD) is a disease spectrum that encompasses highly heterogeneous conditions in terms of clinical phenotypes,

neuropathological features, and genetic underpinnings.¹ FTLD with tauopathy (FTLD-tau) represents up to 40% of all FTLD cases,² and pathogenic mutations in

*Correspondence to: Dr. Jian Wang; Dr. Yi-Min Sun; Dr. Chuan-Tao Zuo, Department of Neurology, Huashan Hospital, Fudan University, 12 Wulumuqi Zhong Road, Shanghai 200040, China; E-mail: wangjian_hs@fudan.edu.cn; ys2504@sina.com; zuochuantao@fudan.edu.cn or Dr. Chuan-Tao PET Center, Huashan Hospital, Fudan University, 518 East Wuzhong Road, Shanghai 200235, China;

Xin-Yue Zhou, Jia-Ying Lu, and Feng-Tao Liu contributed equally to this work.

Chuan-Tao Zuo, Yi-Min Sun, and Jian Wang jointly supervised this work.

Relevant conflicts of interest/financial disclosures: Tzu-Chen Yen is an employee of APRINOIA Therapeutics Co., Ltd (Suzhou, China). All

other authors report no financial relationships and no conflicts of interest with commercial interests. The content of this article represents original work that has not been previously published and is not under consideration for publication elsewhere.

Full financial disclosures and author roles may be found in the online version of this article.

Received: 13 August 2021; **Accepted:** 1 November 2021

Published online in Wiley Online Library
(wileyonlinelibrary.com). DOI: 10.1002/mds.28867

the microtubule-associated protein tau (*MAPT*; OMIM 157140) gene are responsible for the genetic form of FTLD-tau.³ Under physiological conditions, roughly equal amounts of tau isoforms with three (3R) or four repeats (4R) of microtubule-binding domains are produced.⁴ However, the relative abundance of 3R and 4R tau isoforms can be altered by disease-causing *MAPT* mutations, ultimately resulting in 3R, 4R, or 3R + 4R tauopathies.⁵ Specifically, *MAPT* mutations within exon 10 and the surrounding introns, which collectively represent a significant hotspot, have been shown to result in excess 4R tau production.^{6,7}

Recent advances in tau positron emission tomograph (PET) tracers have fostered our ability to identify cerebral tau deposits. Although ¹⁸F-AV-1451 tau PET has been used to image patients who carried at least 10 different *MAPT* mutations, the diagnostic performances have been inconsistent.⁸⁻¹⁴ Although the tracer avidly binds to 3R + 4R tau deposits (which are mainly caused by *MAPT* mutations outside of exon 10), the ability to visualize 4R tau accumulation (which is chiefly elicited by mutations within exon 10) appears more limited.¹⁰ Another traditional tau tracer, ¹¹C-PBB3, has shown good performance for visualizing 4R tau aggregates in patients harboring the *MAPT* N279K variant,¹⁵ but it is clinically limited by its intrinsic metabolic instability and rapid clearance.¹⁶ Although the utility of the second-generation tau radiotracer ¹⁸F-PI-2620 has been investigated in patients with progressive supranuclear palsy (PSP; a 4R tauopathy), whether it might have clinical value in *MAPT* mutation carriers remains unanswered.¹⁷

Previous data suggested that the second-generation tau tracer ¹⁸F-APN-1607 outperforms ¹¹C-PBB3 in terms of signal-to-noise ratio, while having minimal cross-reactivity with monoamine oxidases.¹⁸ In addition, its binding patterns in sporadic FTLD-tau cases have been shown to consistently correlate with neuropathological findings.¹⁸ Nonetheless, the diagnostic performances of ¹⁸F-APN-1607 positron emission tomography/computed tomography (PET/CT) imaging in cases with genetic FTLD-tau caused by *MAPT* mutations have not been thoroughly investigated. Interestingly, a significant cortical and subcortical ¹⁸F-APN-1607 uptake has been recently reported in a patient with behavioral variant frontotemporal dementia (FTD) who harbored a *MAPT* P301L mutation occurring in exon 10.¹⁹ In light of the significant heterogeneity in terms of disease phenotypes and neuropathological features among *MAPT* mutation carriers, the potential value of ¹⁸F-APN-1607 PET/CT imaging should be investigated by taking into account both clinical and genetic findings.

The purpose of this study was twofold. First, we sought to investigate the clinical utility of ¹⁸F-APN-1607 PET/CT in *MAPT* mutation carriers by analyzing a sample of seven patients with different phenotypes. To this

aim, both regional standardized uptake value ratios (SUVRs) and the patterns of tau deposition were thoroughly investigated in a cross-sectional analysis. Second, three patients underwent an imaging follow-up study to assess whether ¹⁸F-APN-1607 tau PET/CT may serve as a potential imaging biomarker of disease progression.

Subjects and Methods

Participants

This study conforms to the tenets of the Declaration of Helsinki and was approved by the Ethics Committee of the Huashan Hospital, Fudan University (Shanghai, China). Written informed consent was obtained from all participants. The study patients were recruited from the Movement Disorders Clinics of the Huashan Hospital, Fudan University, between May 2014 and May 2020. We identified eight patients harboring previously described pathogenic *MAPT* variants.^{15,20-22} One case who did not undergo ¹⁸F-APN-1607 tau PET/CT imaging was excluded; therefore, the final study sample consisted of seven patients. *MAPT* mutation analysis was performed using second-generation sequencing, and all of the identified variants were further confirmed with Sanger sequencing (Supporting Information Fig. S1).²³ Between May 2019 and November 2020, we also included a total of 15 consecutive healthy control subjects with a negative history of neurological or psychiatric disorders.

Clinical Assessments

All patients were scheduled to undergo regular follow-up visits on an annual basis. Variables collected from the study participants and their family members were demographic data, medical history, and clinical manifestations. Patients were considered to have symptoms of FTD when the diagnostic criteria for FTD were met. The motor presentation was categorized as PSP, corticobasal syndrome (CBS), or amyotrophic lateral sclerosis (ALS) according to the currently accepted diagnostic criteria.²⁴⁻³⁰ Cognitive and motor functioning were assessed on each visit.³¹ ¹⁸F-APN-1607 PET/CT scans were scheduled for each patient at the nearest visit after July 2019 (baseline) and during the subsequent visit over a 12-month (± 2 months) time interval. However, patients A-II-2, A-II-3, and B-III-1 were unwilling to receive a follow-up ¹⁸F-APN-1607 PET/CT examination. In addition, patient E-II-2 became uncooperative as a result of a significant clinical deterioration over time.

Image Acquisition and Processing

On completion of clinical assessment, all participants underwent the following imaging studies (see Supporting Information): (1) structural magnetic resonance imaging (MRI), (2) dopamine transporter

imaging with ¹¹C-CFT PET/CT, (3) glucose metabolism imaging with ¹⁸F-FDG PET/CT, and (4) tau imaging with ¹⁸F-APN-1607 PET/CT. All images were obtained on separate days within 1 week of each other. ¹⁸F-APN-1607 tau PET/CT imaging was conducted using a Siemens mCT Flow PET/CT scanner (Siemens, Erlangen, Germany). The procedures have been previously described.³² In brief, the window scanning time was 90–110 min¹⁸ after the intravenous administration of ¹⁸F-APN-1607 (370 MBq), which was prepared in the Huashan Hospital PET center. Images were reconstructed using a 3D ordered-subset expectation maximization algorithm. Individual PET and corresponding T1-weighted MRIs were coregistered using the SPM12 software (<http://www.fil.ion.ucl.ac.uk/spm/software/spm12/>) implemented in MATLAB 9.5 (MathWorks, Natick, MA, USA). The transformation matrices of segmented T1-weighted MRIs were applied to matched PET images into the Montreal Neurological Institute standard space. Normalized images were subsequently smoothed with a Gaussian kernel at a half-maximum with a full width of 6 mm. SUVR maps were obtained using the cerebellar gray matter as the reference region. Mean regional SUVR values were extracted using the following regions of interest (ROIs): 42 cerebral gray matter ROIs identified from the automated anatomical atlas (AAL) three template,³³ 8 cerebral white matter ROIs merged from the AAL-VOI template in the PMOD software (version 4.005,

<http://www.pmod.com>), and 14 predefined subcortical ROIs.³² The hippocampus was excluded from the analysis because of its anatomical contiguity to the choroid plexus.¹⁸ A list of all ROIs examined in the study is provided in Supporting Information Table S1.

Data Analysis

Groups were compared by χ^2 (categorical data) or Student *t* tests (continuous data). Regional SUVR *z* scores were calculated using the following formula: *z* score = (crude SUVR observed in *MAPT* mutation carriers – mean SUVR observed in healthy controls)/standard deviation of SUVR observed in healthy control subjects.

On analyzing ¹⁸F-APN-1607 tau PET images, a SUVR *z* score ≥ 2 standard deviations was used as the criterion to define positive findings. Statistical significance was defined as a two-tailed *P* < 0.05.

Results

Participant Characteristics

A total of seven *MAPT* mutation carriers from five families were included in the study (Fig. 1). The general characteristics of patients and control subjects are shown in Supporting Information Table S2. The clinical features of the study patients were markedly heterogeneous. The clinical, genetic, and imaging data of the seven patients

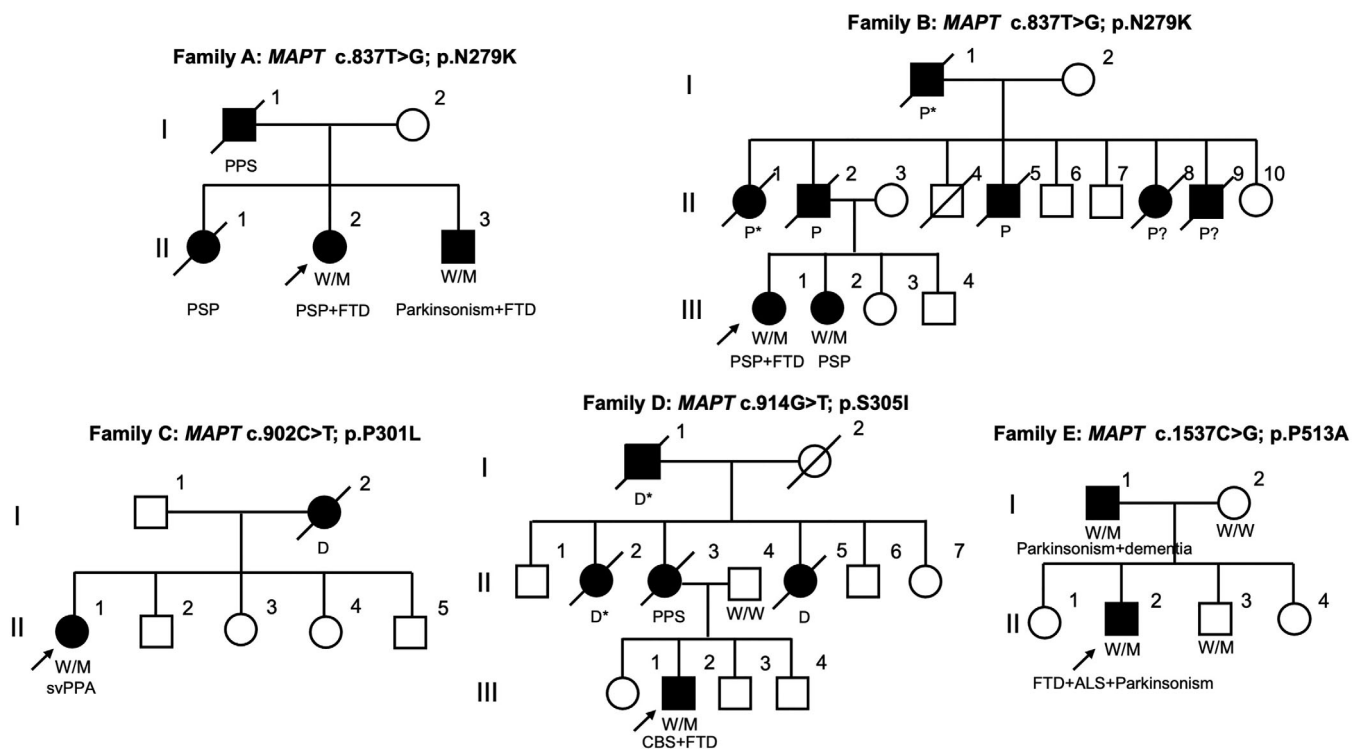


FIG. 1. Family trees showing the distribution of *MAPT* mutations. ALS, amyotrophic lateral sclerosis; CBS, corticobasal syndrome; D, dementia; D*, suspected dementia; FTD, frontotemporal dementia; M, mutant; P, parkinsonism; P*, suspected parkinsonism; PPS, Parkinson's plus syndrome; PSP, progressive supranuclear palsy; W, wild-type.

TABLE 1 General characteristics of the seven MAPT mutation carriers

	Patient A-II-2	Patient A-II-3	Patient B-III-1	Patient B-III-2	Patient C-II-1	Patient D-III-2	Patient E-II-2
Genetic data							
MAPT mutation	N279K	N279K	N279K	N279K	P301L	S305I	P513A
Expected tau isoform(s)	4R	4R	4R	4R	4R	4R	3R + 4R
General characteristics							
Clinical diagnosis at baseline	Probable PSP + FTD	Parkinsonism	Probable PSP + FTD	Suggestive of PSP	FTD	Possible CBS	Parkinsonism + probable ALS + FTD
Clinical diagnosis at follow-up	Probable PSP + FTD	Parkinsonism + FTD	NA	Probable PSP	FTD	Probable CBS + FTD	NA
Age at onset (y)	48	50	44	43	55	35	41
Disease duration (baseline/follow-up) (mo)	100 ^a /123	6 ^a /29	43 ^a /NA	21 ^a /35 ^a	24 ^a /36 ^a	9 ^a /19 ^a	38 ^a /NA
Baseline imaging features							
MRI							
Frontal and temporal atrophy	+	+	+	+	+	-	+
FDG PET/CT imaging							
Frontal hypometabolism	NA	+	+	+	+	+	+
Temporal hypometabolism	NA	+	+	-	+	-	-
Midbrain hypometabolism	NA	+	+	+	-	+	-
DAT PET/CT imaging							
Anterior putamen alterations	+	+	+	+	+	+	-
Posterior putamen alterations	+	+	+	+	+	±	±
Caudate alterations	+	+	+	+	+	-	+

^aCalculated at the time of ¹⁸F-APN-1607 PET imaging. +, positive; -, negative; ±, suspected; ALS, amyotrophic lateral sclerosis; CBS, corticobasal syndrome; DAT, dopamine transporter; FDG, fluorodeoxyglucose; FTD, frontotemporal dementia; MRI, magnetic resonance imaging; NA, not available; PET/CT, positron emission tomography/computed tomography; PSP, progressive supranuclear palsy.

are depicted in Table 1 and Supporting Information Table S3, which present the various clinical symptoms in chronological order as they appeared. Figure 2 shows the results of ¹⁸F-APN-1607 tau PET imaging, whereas ¹⁸F-FDG PET and ¹¹C-CFT PET images are provided in Supporting Information Fig. S2.

¹⁸F-APN-1607 Imaging in MAPT Mutation Carriers: Baseline Findings

MAPT N279K (Families A and B)

Four patients (A-II-2, A-II-3, B-III-1, and B-III-2) from two different families (A and B) carried a MAPT N279K mutation. All showed parkinsonism at the time of disease onset, and some of the core symptoms of PSP

were observed later among patients A-II-2, B-III-1, and B-III-2. Notably, patients A-II-2, A-II-3, and B-III-1 developed FTD symptoms during their clinical course, which was accompanied by severe widespread cortical accumulation of tau deposits.

Patient A-II-2, who originally presented with parkinsonism, subsequently showed typical symptoms of PSP, accompanied by apraxia of speech. On ¹⁸F-APN-1607 tau PET imaging, there was diffuse tracer uptake, especially in the subcortical regions, including striatum, putamen, pallidum, subthalamic nucleus (STN), tegmentum, red nucleus (RN), raphe nuclei, and dentate. The cerebral cortex and all of the white matter regions also showed extensive involvement. Patient A-II-3 presented with symmetrical akinesia-rigid parkinsonism. At

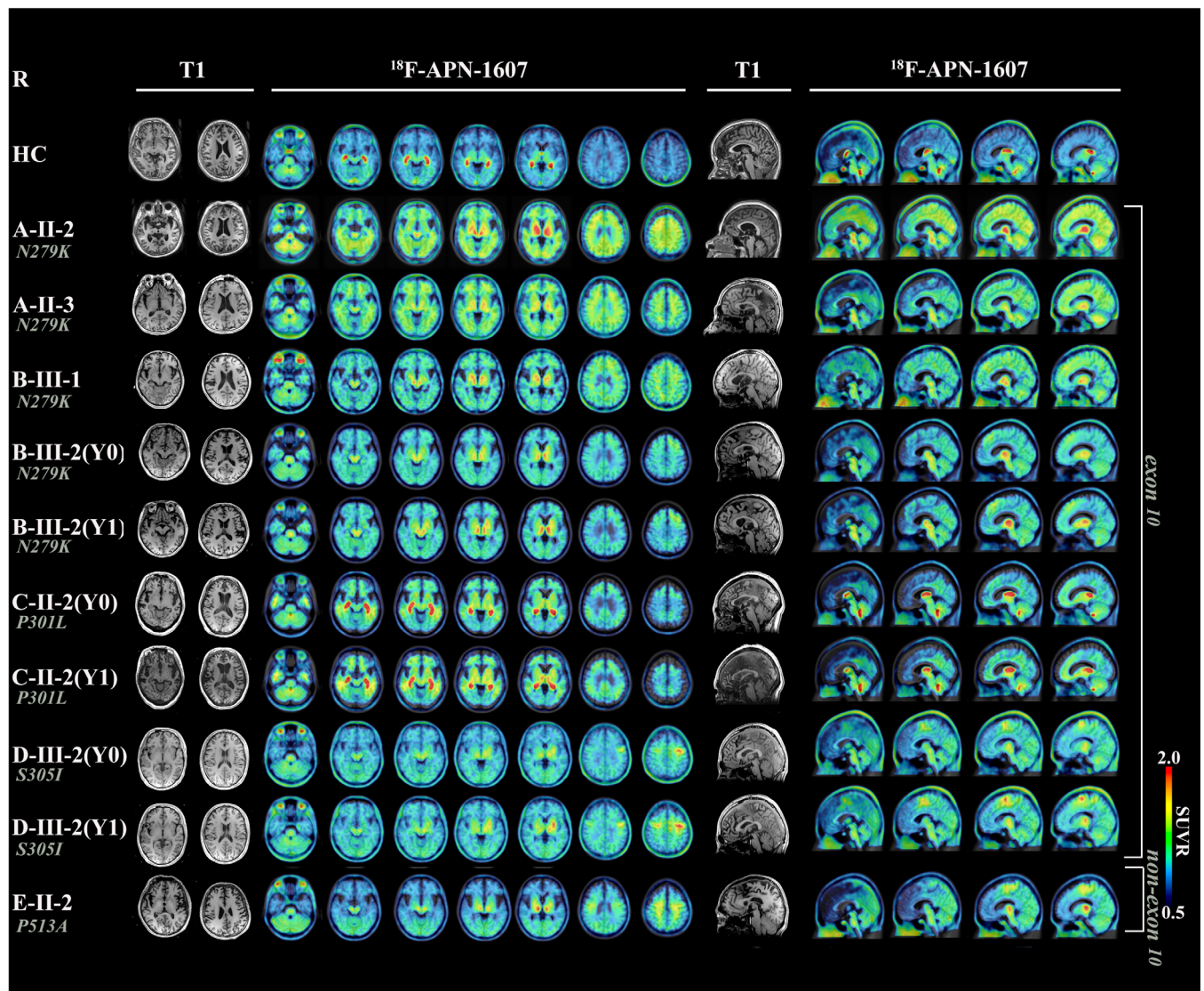


FIG. 2. ¹⁸F-APN-1607 binding patterns observed in MAPT mutation carriers and healthy control subjects: baseline and follow-up data. Each patient is presented separately; the MAPT mutation identified for each case is marked in italics. Y0 denotes baseline findings, whereas Y1 refers to follow-up findings. The patterns of tau depositions were heterogeneous across different MAPT mutations. Compared with baseline values, the three patients who were longitudinally followed up (B-III-2, C-II-1, and D-III-2) showed an increased tau burden over time. HC, healthy control subject; R, right; SUVR, standardized uptake value ratio. [Color figure can be viewed at wileyonlinelibrary.com]

baseline, an increased tracer uptake was observed in subcortical regions, including bilateral putamen and pallidum and right STN and raphe nuclei, as well as in the cortex and corresponding white matter. Baseline ¹⁸F-APN-1607 tau PET imaging also showed extensive tau deposits in the left locus ceruleus, a finding that may account for the significant deterioration in the patient's global cognition and language fluency over a 2-year follow-up.

Patient B-III-1 was diagnosed with probable PSP plus FTD. Symptoms of FTD, including behavioral and language deficits, developed over a 3-year period. On ¹⁸F-APN-1607 tau PET imaging, a markedly high tracer uptake was observed in the frontoparietal cortex; this was especially evident in the left precentral, superior, and middle frontal gyrus, as well as in the bilateral superior medial frontal gyrus. Tau deposits were also evident in subcortical regions, including the right putamen, midbrain, and RN, as well as in the bilateral substantia nigra (SN), pallidum, STN, and tegmentum. Patient B-III-2 presented right-dominant parkinsonian symptoms at onset. A diagnosis of PSP was suspected

at baseline because of predominant postural instability. Baseline ¹⁸F-APN-1607 tau PET imaging showed tau deposits in the left STN, SN, tegmentum, RN, and raphe nuclei. Semiquantitative analysis failed to identify positive tau aggregates in the cortex of patient B-III-2. Consistently, FTD symptoms (eg, personality changes and nonfluent speech) were absent at the time of clinical assessment. Over a 35-month follow-up, there was evidence of oculomotor dysfunction, but FTD symptoms remained negative. After an additional ¹⁸F-APN-1607 tau PET scan, her diagnosis was changed to probable PSP without FTD.

MAPT P301L (Family C)

Patient C-II-1, who harbored a *MAPT* P301L mutation, was diagnosed with FTD (subtype: semantic variant primary progressive aphasia) at the age of 57 years. There was no evidence of movement disorders. Semiquantitative analysis of ¹⁸F-APN-1607 PET/CT imaging findings showed that positive tau aggregates were limited to the bilateral thalamus. Temporal involvement is

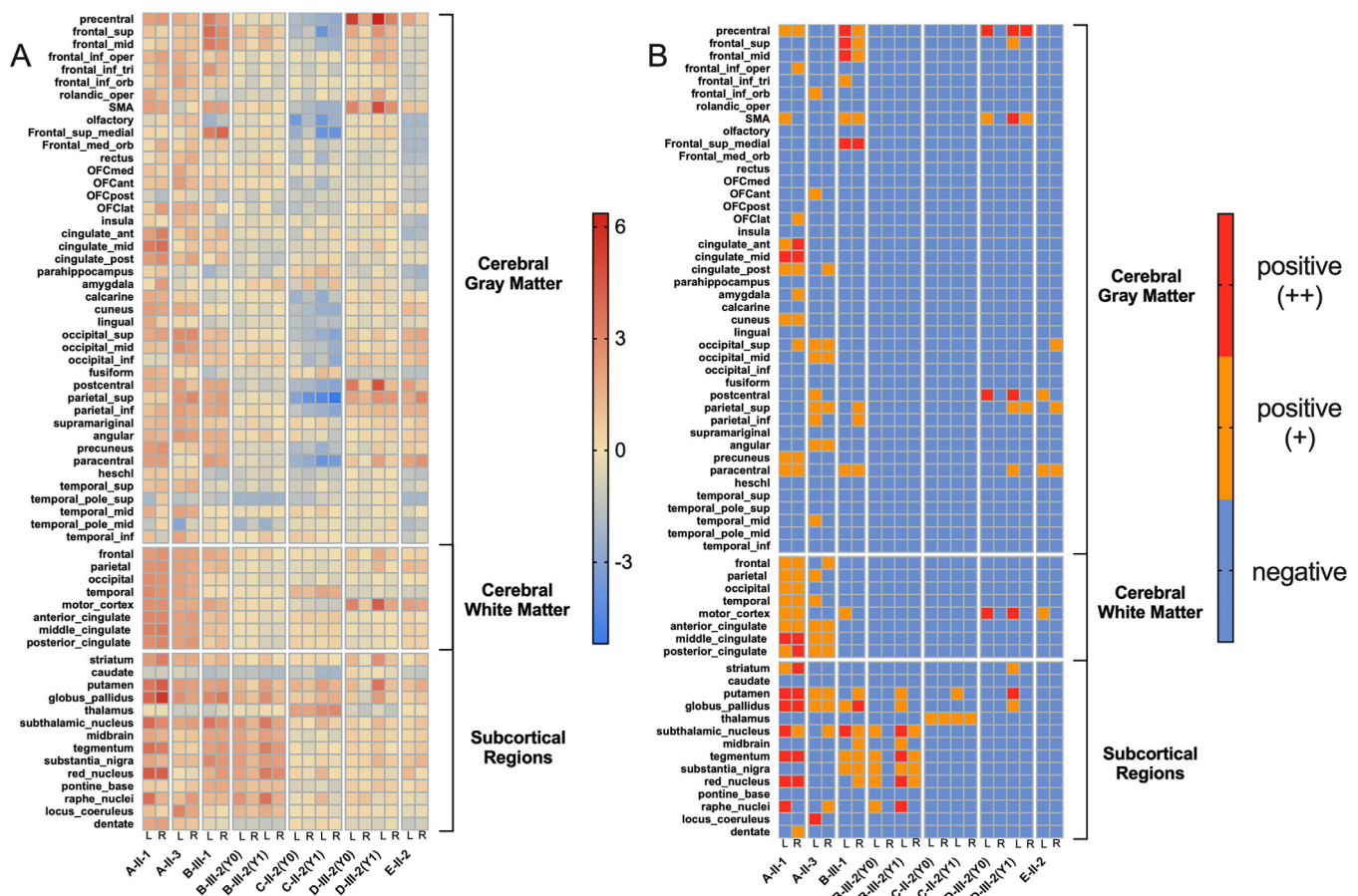


FIG. 3. Heatmaps of regional z scores in the seven *MAPT* mutation carriers: baseline and follow-up data. Y0 denotes baseline findings, whereas Y1 refers to follow-up findings. (A) Original z scores. (B) Negative regions (z scores <2 standard deviations) are marked in blue; mildly positive regions (z scores ≥2 and <3 standard deviations) are denoted in orange; definitely positive regions (z scores ≥3 standard deviations) are marked in red. [Color figure can be viewed at wileyonlinelibrary.com]

a disease-specific anatomic feature of semantic variant primary progressive aphasia. Although on visual assessment positive signals were identified in the temporal white matter, the SUVR z score (1.272) did not meet the positivity criteria for tau aggregates. On follow-up examinations, the patient had behavioral disturbances; however, her motor function remained normal.

MAPT S305I (Family D)

Patient D-III-2, who harbored an *MAPT* S305I mutation, developed right hand apraxia accompanied by a reduced arm swing at the age of 35 years. A diagnosis of CBS was suspected. ^{18}F -APN-1607 PET/CT imaging findings at baseline demonstrated the presence of tau accumulation in the precentral and postcentral gyrus, the supplementary motor area, and the corresponding motor cortex white matter. A significant asymmetry was evident (predominance observed on the contralateral side with respect to the initially affected side). On a 14-month follow-up, he had rigid-akinesia parkinsonism, dystonia, and myoclonus with significant right-side predominance. Because of the presence of agrammatism and reduced language fluency, he was diagnosed with probable CBS combined with FTD.

MAPT P513A (Family E)

Patient E-II-2, who harbored a *MAPT* P513A mutation, presented with asymmetrical parkinsonism, muscle weakness, and mild cognitive impairment at the age of 41 years. Although electromyogram findings were initially unremarkable, both bulbar palsy and behavioral symptoms were evident. At the age of 43 years, the results of electromyogram indicated motor neuron loss in the biceps and paravertebral muscles (T10 level). A diagnosis of FTD-ALS-parkinsonism was made. The results of ^{18}F -APN-1607 PET/CT imaging showed cortical tau accumulation, most notably in the paracentral gyrus, postcentral gyrus, certain portions of the parietal and occipital gyrus, as well as in the motor cortex white matter.

^{18}F -APN-1607 PET/CT Imaging: Follow-Up Findings

Three *MAPT* mutation carriers (patients B-III-2, C-II-2, and D-III-2) received follow-up ^{18}F -APN-1607 PET/CT imaging at 14, 12, and 10 months from the initial scan, respectively. All three patients showed a significant clinical deterioration, with worsening of the original symptoms and/or the onset of new manifestations that were initially absent (Table 1 and Supporting Information Table S3). These findings were paralleled by a trend of increased tau burden over time. On visual examination, follow-up ^{18}F -APN-1607 PET findings showed an increasing burden of tau accumulation over time in all cases. In addition, regions characterized by

the presence of tau aggregates at baseline showed a trend toward increasing SUVR values at follow-up. Remarkably, certain regions that did not show tau deposits at baseline became positive during the course of follow-up (Figs. 2 and 3). Specifically, patient B-III-2 showed increasing tau deposits in midline structures involving the putamen, pallidum, and midbrain, as well as the STN, tegmentum, SN, and RN. These imaging findings were paralleled by an obvious deterioration in terms of motor dysfunction. On visual examination, the follow-up ^{18}F -APN-1607 PET/CT scan of patient C-II-2 showed an enlargement of tau deposits, which were also characterized by an increased tracer uptake over time (SUVR z scores at baseline and follow-up: 1.272 and 1.868, respectively). In addition, quantitative analysis demonstrated positive tau aggregates in the left putamen, which were initially absent. The second ^{18}F -APN-1607 PET/CT scan of patient D-III-2 showed novel tau deposits in various initially unaffected areas (eg, basal ganglia and frontoparietal regions, mainly in the left side). These imaging results were accompanied by newly developed contralateral parkinsonism and a significant deterioration in terms of language dysfunction.

Discussion

This is, to our knowledge, the first study to provide an in-depth analysis of ^{18}F -APN-1607 PET/CT findings in patients with FTLD-tau caused by different *MAPT* mutations, as well as the first to apply this imaging modality to describe the longitudinal changes of tau accumulation occurring over time in this rare and heterogeneous clinical entity.

Once we had obtained baseline evidence indicating a significant ^{18}F -APN-1607 uptake with high-contrast signals in all of the seven participants, we then analyzed whether the location of pathogenic *MAPT* mutations (ie, within exon 10 versus outside of exon 10) could be related to the observed ^{18}F -APN-1607 PET/CT imaging findings. We found that the anatomical localization of tau deposits varied according to the clinical phenotypes of FTLD-tau as a result of different *MAPT* mutations. In addition, on analysis of the follow-up ^{18}F -APN-1607 PET/CT images obtained from three patients carrying pathogenic exon 10 mutations, we identified worsening trends in terms of tau accumulation over time, which were noticeably paralleled by a significant clinical deterioration.

The exon 10 *MAPT* mutations observed in this study (N279K, P301L, and S305I) were expected to accelerate the production of 4R tau isoforms. Both first- and second-generation tau tracers have been investigated in 4R tauopathies, with inconsistent performances. Although previous ^{18}F -AV-1451 PET/CT studies focusing

on patients who carried the same mutations showed discrepant findings, most found either negative or mild tracer uptake (Supporting Information Table S4).^{8-10,12} In addition, inconsistencies were also observed when ¹⁸F-AV-1451 imaging results were analyzed with respect to neuropathological findings. Although an autopsy study conducted in a S305I mutation carrier showed that cerebral areas characterized by elevated ¹⁸F-AV-1451 uptake corresponded to regions with a severe burden of tau pathology,¹³ the pattern of ¹⁸F-AV-1451 accumulation in a P301L mutation carrier did not correlate with tau brain deposits identified on postmortem analysis.⁸ Another traditional tracer (¹¹C-PBB3) has been investigated in FTLD-tau patients harboring *MAPT* exon 10 mutations and was found to successfully image 4R tauopathies.¹⁵ Unfortunately, its clinical applications are severely limited by the intrinsic metabolic instability, rapid clearance, and potential off-target binding.³² The second-generation tau tracer ¹⁸F-PI-2620 is also characterized by high affinity to 4R tau isoforms in patients with PSP, but its potential utility in *MAPT*-related FTLD-tau deserves further scrutiny.¹⁷ In our investigation conducted using ¹⁸F-APN-1607 as tau PET tracer, all cases harboring exon 10 *MAPT* mutations invariably showed high-contrast signals despite varying clinical phenotypes. These consistent results may reflect a higher affinity of ¹⁸F-APN-1607 compared with ¹⁸F-AV-1451 for 4R tau isoforms.¹⁹ Although these findings are preliminary, they call attention to the importance of appropriately selecting the most suitable tau PET tracer in *MAPT* mutation carriers.

Subcortical tau aggregates, especially in the basal ganglia, were identified in the majority of our *MAPT* mutation carriers. In accordance with our findings, previous neuropathological studies in *MAPT*-related FTLD indicated the presence of varying degrees of tau deposition in the basal ganglia even in patients who did not show movement disorders.^{13,21,34-37} However, tracer uptake in the basal ganglia should be interpreted with caution because it may result from off-target binding. Notably, more than 50% of *MAPT* mutation carriers had evidence of prominent white matter tau pathology, a finding that is strikingly different from the predominant localization of tau deposits in the gray matter occurring in Alzheimer's disease.¹⁵ Previous neuroimaging and neuropathological investigations have consistently shown that *MAPT*-related FTLD-tau is characterized by a significant white matter burden.^{38,39} Further investigations with larger sample sizes are required to investigate in greater detail the longitudinal trajectories of tau deposition in the white matter of *MAPT* mutation carriers.

On visual examination, the topographical distribution of cortical ¹⁸F-APN-1607 uptake was largely similar to regional hypometabolism observed on ¹⁸F-FDG PET images. Interestingly, the patterns of tau deposits in the brain were found to predominantly reflect the

clinical phenotype rather than the presence of specific mutations. Among the *MAPT* N279K mutation carriers included in our study, cases with widespread cortical involvement showed severe clinical phenotypes (ie, FTD symptoms including personality changes, and language impairment); conversely, patient B-III-2, who exhibited a more limited involvement of the frontal cortex, had milder symptoms. This observation may also explain the discrepancies between our data and previous ¹⁸F-AV-1451 PET investigations focusing on *MAPT* S305I mutation carriers. The application of ¹⁸F-AV-1451 PET imaging in two patients with behavioral variant FTD harboring this mutation showed symmetrical tau deposition in the frontal, temporal cortex, and corresponding white matter.^{9,13} Different from the previously reported phenotype, our D-III-2 patient showed symptoms of CBS (predominantly in the right side). Accordingly, a significant asymmetrical involvement of the primary motor cortex was observed. This pattern was consistent with those previously reported for sporadic CBS both in neuropathology⁴⁰ and in ¹⁸F-APN-1607 tau PET/CT imaging studies.¹⁸

The *MAPT* P513A mutation, which is located outside of exon 10, has been originally described in a family with nonfluent variant primary progressive aphasia²² and subsequently identified in patients with Alzheimer's disease.⁴¹ The study participant harboring this mutation (E-II-1) had symptoms of ALS, which is a relatively uncommon manifestation of *MAPT* mutations being predominantly linked to TAR DNA binding protein 43 (TDP-43) pathology.⁴²⁻⁴⁴ Although the neuropathological impact of this mutation has yet to be determined, we hypothesize that it can lead to cortical and subcortical tau deposits consisting of both 3R and 4R isoforms. This would be in accordance with previous observations reported for patients with different mutations outside of exon 10.⁴⁵ Consistent with published findings obtained from patients with ALS,⁴⁶⁻⁴⁸ the results of ¹⁸F-APN-1607 PET/CT imaging in our *MAPT* P513A mutation carrier showed tau deposits affecting the motor cortex and the somatosensory cortex. However, caution should be exercised in interpreting these results in light of the potential off-target binding of ¹⁸F-APN-1607 to TDP-43.

Data concerning the longitudinal changes of tau deposition occurring in carriers of *MAPT* mutations over time are currently limited.⁴⁹ Our study focused on this issue by analyzing consecutive ¹⁸F-APN-1607 PET/CT images collected in three carriers of *MAPT* exon 10 mutations who presented with PSP and CBS-like phenotypes. Patients who received follow-up imaging demonstrated a worsening tau burden over time, which was paralleled by a significant clinical deterioration. Albeit preliminary, these findings provide pilot evidence on the potential utility of ¹⁸F-APN-1607 PET/CT findings for monitoring the clinical course of 4R

tauopathies caused by *MAPT* mutations. However, the number of patients who underwent longitudinal imaging was limited, and larger scaled studies with longer follow-up duration are necessary to confirm our findings. Further research is also needed to evaluate the prognostic role of ^{18}F -APN-1607 PET/CT imaging in FTLD-tau with *MAPT* mutations.

Our findings should be interpreted in the context of several limitations. First, we cannot rule out an *in vivo* cross-reactivity of ^{18}F -APN-1607 to monoamine oxidases or non-tau protein aggregates. Second, the ROIs identified from the purpose of the study were drawn from several public templates. In certain cases, it would be possible that tau deposits could be limited to a small portion of the ROI. Consequently, regional SUVR values that represent the average range of tau aggregates might not accurately reflect the tau burden within the ROI. We also acknowledge that tracer uptake might have occurred in the reference region located in the cerebellum, potentially leading to an underestimation of regional SUVR values. Third, because poor patient cooperation was relatively common in our cohort, we chose to rely on late-phase static imaging only,¹⁸ and no correction for blood flow or arterial input was applied. Future studies using a dynamic acquisition protocol will be required to shed further light on the clinical value of ^{18}F -APN-1607 PET/CT imaging in *MAPT* mutation carriers. Fourth, the small sample size posed a limitation regarding the ability to generalize our conclusions, as well as our ability to explore the relationships between regional tau deposition and clinical symptoms. In this scenario, replication in independent samples is paramount for ensuring external validity. Fifth, we acknowledge that tau burden might have been underestimated in *MAPT* mutation carriers because patients were significantly younger than the healthy control subjects. Finally, because we had no postmortem data concerning brain tau deposition, we were unable to analyze the correlations between the results of ^{18}F -APN-1607 PET/CT imaging and pathological findings. Future autopsy studies in *MAPT* mutation carriers who had undergone ^{18}F -APN-1607 PET/CT imaging should work to address this limitation.

Conclusions

Our data represent a promising step in understanding the clinical usefulness of ^{18}F -APN-1607 PET/CT imaging for detecting the burden of tau accumulation in *MAPT* mutation carriers. This imaging modality may be applied for identifying 4R tau deposits during baseline work-up examinations. In addition, our preliminary follow-up data suggest the potential value of ^{18}F -APN-1607 PET/CT for monitoring the longitudinal

trajectories of patients with FTLD-tau caused by *MAPT* mutations. ■

Acknowledgments: J.W. received research funding from Shanghai Municipal Science and Technology Major Project (Grants 2018SHZDZX01, 2017SHZDZX01, and 21S31902200), ZJ Lab, and Shanghai Center for Brain Science and Brain-Inspired Technology, as well as the National Nature Science Foundation of China (Grants 82171421, 91949118, and 81771372). C.-T.Z. was supported by the National Nature Science Foundation of China (Grants 81971641, 81671239, and 8201002), Research Project of Shanghai Health Commission (Grant 2020YJZX0111), and Clinical Research Plan of Shanghai Shen Kang Hospital Development Center (Grant SHDC2020CR1038B). We are grateful to APRINOIA Therapeutics Co., Ltd (Suzhou, China) for providing the tosylate precursor used for ^{18}F -APN-1607 radiosynthesis. The authors thank all patients and family members who were involved in this research. None of the study participants received financial incentives.

Data Availability Statement

The data that support the findings of this study are available on request from the corresponding author.

References

1. Kertesz A, McMonagle P, Blair M, Davidson W, Munoz DG. The evolution and pathology of frontotemporal dementia. *Brain* 2005; 128(Pt 9):1996–2005.
2. Panza F, Lozupone M, Seripa D, et al. Development of disease-modifying drugs for frontotemporal dementia spectrum disorders. *Nat Rev Neurol* 2020;16(4):213–228.
3. Forrest SL, Kril JJ, Stevens CH, et al. Retiring the term FTDP-17 as *MAPT* mutations are genetic forms of sporadic frontotemporal tauopathies. *Brain* 2018;141(2):521–534.
4. Chen S, Townsend K, Goldberg TE, Davies P, Conejero-Goldberg C. *MAPT* isoforms: differential transcriptional profiles related to 3R and 4R splice variants. *J Alzheimers Dis* 2010;22(4): 1313–1329.
5. Ghetti B, Oblak AL, Boeve BF, Johnson KA, Dickerson BC, Goedert M. Invited review: frontotemporal dementia caused by microtubule-associated protein tau gene (*MAPT*) mutations: a chameleon for neuropathology and neuroimaging. *Neuropathol Appl Neurobiol* 2015;41(1):24–46.
6. Park SA, Ahn SI, Gallo JM. Tau mis-splicing in the pathogenesis of neurodegenerative disorders. *BMB Rep* 2016;49(8):405–413.
7. McCarthy A, Lonergan R, Olszewska DA, et al. Closing the tau loop: the missing tau mutation. *Brain* 2015;138(Pt 10):3100–3109.
8. Marquié M, Normandin MD, Meltzer AC, et al. Pathological correlations of [^{18}F]-AV-1451 imaging in non-alzheimer tauopathies. *Ann Neurol* 2017;81(1):117–128.
9. Tsai RM, Bejanin A, Lesman-Segev O, et al. (^{18}F)-flortaucipir (AV-1451) tau PET in frontotemporal dementia syndromes. *Alzheimers Res Ther* 2019;11(1):13
10. Jones DT, Knopman DS, Graff-Radford J, et al. In vivo ^{18}F -AV-1451 tau PET signal in *MAPT* mutation carriers varies by expected tau isoforms. *Neurology* 2018;90(11):e947–e954.
11. Bevan Jones WR, Cope TE, Passamonti L, et al. [(^{18}F)]AV-1451 PET in behavioral variant frontotemporal dementia due to *MAPT* mutation. *Ann Clin Transl Neurol* 2016;3(12):940–947.
12. Wolters EE, Papma JM, Verfaillie SCJ, et al. [(^{18}F)]Flortaucipir PET across various *MAPT* mutations in presymptomatic and symptomatic carriers. *Neurology* 2021;97(10):e1017–e1030.
13. Soleimani-Meigooni DN, Iaccarino L, La Joie R, et al. ^{18}F -flortaucipir PET to autopsy comparisons in Alzheimer's disease and other neurodegenerative diseases. *Brain* 2020;143(11):3477–3494.
14. Smith R, Puschmann A, Schöll M, et al. ^{18}F -AV-1451 tau PET imaging correlates strongly with tau neuropathology in *MAPT* mutation carriers. *Brain* 2016;139(Pt 9):2372–2379.

15. Ikeda A, Shimada H, Nishioka K, et al. Clinical heterogeneity of frontotemporal dementia and Parkinsonism linked to chromosome 17 caused by MAPT N279K mutation in relation to tau positron emission tomography features. *Mov Disord* 2019;34(4):568–574.
16. Kimura Y, Ichise M, Ito H, et al. PET quantification of tau pathology in human brain with 11C-PBB3. *J Nucl Med* 2015;56(9):1359–1365.
17. Brendel M, Barthel H, van Eimeren T, et al. Assessment of 18F-PI-2620 as a biomarker in progressive supranuclear palsy. *JAMA Neurol* 2020;77(11):1408–1419.
18. Tagai K, Ono M, Kubota M, et al. High-contrast in vivo imaging of tau pathologies in Alzheimer's and non-Alzheimer's disease tauopathies. *Neuron* 2021;109(1):42–58.e48.
19. Su Y, Fu J, Yu J, et al. Tau PET imaging with [18F]PM-PBB3 in frontotemporal dementia with MAPT mutation. *J Alzheimers Dis* 2020;76(1):149–157.
20. Delisle M-B, Murrell JR, Richardson R, et al. A mutation at codon 279 (N279K) in exon 10 of the Tau gene causes a tauopathy with dementia and supranuclear palsy. *Acta Neuropathol* 1999;98(1):62–77.
21. Kovacs GG, Pittman A, Revesz T, et al. MAPT S305I mutation: implications for argyrophilic grain disease. *Acta Neuropathol* 2008;116(1):103–118.
22. Tang M, Gu X, Wei J, et al. Analyses MAPT, GRN, and C9orf72 mutations in Chinese patients with frontotemporal dementia. *Neurobiol Aging* 2016;46(235):e211–e235.
23. Sun YM, Yu HL, Zhou XY, et al. Disease progression in patients with Parkin-related Parkinson's disease in a longitudinal cohort. *Mov Disord* 2021;36(2):442–448.
24. Bang J, Spina S, Miller BL. Frontotemporal dementia. *Lancet* 2015;386(10004):1672–1682.
25. Rascovsky K, Hodges JR, Kipps CM, et al. Diagnostic criteria for the behavioral variant of frontotemporal dementia (bvFTD): current limitations and future directions. *Alzheimer Dis Assoc Disord* 2007;21(4):S14–S18.
26. Bensimon G, Ludolph A, Agid Y, Vidailhet M, Payan C, Leigh PN. Riluzole treatment, survival and diagnostic criteria in Parkinson plus disorders: the NNIPPS study. *Brain* 2009;132(Pt 1):156–171.
27. Gorno-Tempini ML, Hillis AE, Weintraub S, et al. Classification of primary progressive aphasia and its variants. *Neurology* 2011;76(11):1006–1014.
28. Armstrong MJ, Litvan I, Lang AE, et al. Criteria for the diagnosis of corticobasal degeneration. *Neurology* 2013;80(5):496–503.
29. Höglinger GU, Respondek G, Stamelou M, et al. Clinical diagnosis of progressive supranuclear palsy: the movement disorder society criteria. *Mov Disord* 2017;32(6):853–864.
30. Brooks BR, Miller RG, Swash M, Munsat TL. El Escorial revisited: revised criteria for the diagnosis of amyotrophic lateral sclerosis. *Amyotroph Lateral Scler Other Motor Neuron Disord* 2000;1(5):293–299.
31. Tang Y, Liang X, Han L, et al. Cognitive function and quality of life in Parkinson's disease: a cross-sectional study. *J Parkinsons Dis* 2020;10(3):1209–1216.
32. Li L, Liu FT, Li M, et al. Clinical utility of (18) F-APN-1607 tau PET imaging in patients with progressive supranuclear palsy. *Mov Disord* 2021;36(10):2314–2323. <https://doi.org/10.1002/mds.28672>
33. Rolls ET, Huang CC, Lin CP, Feng J, Joliot M. Automated anatomical labelling atlas 3. *Neuroimage* 2020;206:116189
34. Borrego-Écija S, Morgado J, Palencia-Madrid L, et al. Frontotemporal dementia caused by the P301L mutation in the MAPT gene: clinicopathological features of 13 cases from the same geographical origin in Barcelona, Spain. *Dement Geriatr Cogn Disord* 2017;44(3–4):213–221.
35. Tacic P, Sanchez-Contreras M, DeTure M, et al. Clinicopathologic heterogeneity in frontotemporal dementia and parkinsonism linked to chromosome 17 (FTDP-17) due to microtubule-associated protein tau (MAPT) p.P301L mutation, including a patient with globular glial tauopathy. *Neuropathol Appl Neurobiol* 2017;43(3):200–214.
36. Arima K, Kowalska A, Hasegawa M, et al. Two brothers with frontotemporal dementia and Parkinsonism with an N279K mutation of the tau gene. *Neurology* 2000;54(9):1787–1795.
37. Wszolek ZK, Pfeiffer RF, Bhatt MH, et al. Rapidly progressive autosomal dominant parkinsonism and dementia with pallido-pontonigral degeneration. *Ann Neurol* 1992;32(3):312–320.
38. Chen Q, Boeve BF, Schwarz CG, et al. Tracking white matter degeneration in asymptomatic and symptomatic MAPT mutation carriers. *Neurobiol Aging* 2019;83:54–62.
39. McMillan CT, Irwin DJ, Avants BB, et al. White matter imaging helps dissociate tau from TDP-43 in frontotemporal lobar degeneration. *J Neurol Neurosurg Psychiatry* 2013;84(9):949–955.
40. Arakawa A, Saito Y, Seki T, et al. Corticobasal degeneration with deep white matter lesion diagnosed by brain biopsy. *Neuropathology* 2020;40(3):287–294.
41. Giau VV, Senanarong V, Bagyinszky E, An SSA, Kim S. Analysis of 50 neurodegenerative genes in clinically diagnosed early-onset Alzheimer's disease. *Int J Mol Sci* 2019;20(6):1514.
42. Zarranz JJ, Ferrer I, Lezcano E, et al. A novel mutation (K317M) in the MAPT gene causes FTDP and motor neuron disease. *Neurology* 2005;64(9):1578–1585.
43. Štrafela P, Pleško J, Magdič J, et al. Familial tauopathy with P364S MAPT mutation: clinical course, neuropathology and ultrastructure of neuronal tau inclusions. *Neuropathol Appl Neurobiol* 2018;44(6):550–562.
44. Di Fonzo A, Ronchi D, Gallia F, et al. Lower motor neuron disease with respiratory failure caused by a novel MAPT mutation. *Neurology* 2014;82(22):1990–1998.
45. Spina S, Schonhaut DR, Boeve BF, et al. Frontotemporal dementia with the V337M MAPT mutation: tau-PET and pathology correlations. *Neurology* 2017;88(8):758–766.
46. Qiu T, Zhang Y, Tang X, et al. Precentral degeneration and cerebellar compensation in amyotrophic lateral sclerosis: a multimodal MRI analysis. *Hum Brain Mapp* 2019;40(12):3464–3474.
47. Thorns J, Jansma H, Peschel T, et al. Extent of cortical involvement in amyotrophic lateral sclerosis – an analysis based on cortical thickness. *BMC Neurol* 2013;13(1):148
48. Höffken O, Schmelz A, Lenz M, et al. Excitability in somatosensory cortex correlates with motoric impairment in amyotrophic lateral sclerosis. *Amyotroph Lateral Scler Frontotemporal Degener* 2019;20(3–4):192–198.
49. Convery RS, Jiao J, Clarke MTM, et al. Longitudinal ((18)F)AV-1451 PET imaging in a patient with frontotemporal dementia due to a Q351R MAPT mutation. *J Neurol Neurosurg Psychiatry* 2020;91(1):106–108.

Supporting Data

Additional Supporting Information may be found in the online version of this article at the publisher's web-site.

SGML and CITI Use Only
DO NOT PRINT

Author Roles

1. Research Project: A. Conception, B. Organization, C. Execution;
2. Statistical Analysis: A. Design, B. Execution, C. Review and Critique;
3. Manuscript: A. Writing of the First Draft, B. Review and Critique.

X.-Y. Zhou: 1A, 1B, 1C, 2A, 2B, 2C, 3A, 3B

J.-Y. Lu: 1A, 1B, 1C, 2A, 2B, 2C, 3A, 3B

F.-T. Liu: 1A, 1B, 1C, 2A, 2B, 2C, 3A, 3B

P. Wu: 1A, 1B, 1C, 2A, 2C, 3B

J. Zhao: 1A, 1B, 1C, 2A, 2C, 3B

Z.-Z. Ju: 1A, 1B, 1C, 2A, 2C, 3B

Y.-L. Tang: 1A, 1B, 1C, 2A, 2C, 3B

Q.-Y. Shi: 1A, 1B, 1C, 2A, 2C, 3B

H.-M. Lin: 1A, 1B, 1C, 2A, 2C, 3B

J.-J. Wu: 1A, 1B, 1C, 2C, 3B

T.-C. Yen: 1A, 1B, 1C, 2C, 3B

C.-T. Zuo: 1A, 1B, 1C, 2C, 3B

Y.-M. Sun: 1A, 1B, 1C, 2C, 3B

J. Wang: 1A, 1B, 1C, 2C, 3B

Financial Disclosures

Tzu-Chen Yen is an employee of APRINOIA Therapeutics Co., Ltd (Suzhou, China). All other authors report no financial relationships and no conflicts of interest with commercial interests.